Supercontinuum Generation at 1.55 μm in a Silicon Nanowire Embedded Photonic Crystal Fiber

E. Gunasundari[1], **Abdosllam M. Abobaker**[2], **K. Senthilnathan**[1], **S. Sivabalan**[3], **K. Nakkeeran**[4], **and P. Ramesh Babu**[1]

[1]Photonics, Nuclear and Medical Physics Division, School of Advanced Sciences
VIT University, Vellore 632 014, India
[2]Department of Communications Engineering, College of Electronic Technology, Bani Walid, Libya
[3]School of Electrical Engineering, VIT University, Vellore 632 014, India
[4]School of Engineering, University of Aberdeen, Aberdeen AB24 3UE, UK

Abstract— In this paper, we design an elliptical silicon nanowire embedded photonic crystal fiber (SN-PCF) using fully vectorial finite element method. Further, we analyze the various optical properties, namely, waveguide dispersion, birefringence, fractional power inside the core and effective nonlinearity by varying the ellipticity for a wide range of wavelengths from 0.8 to 1.8 μm. The proposed structure exhibits a high birefringence of 0.4815 for a small ellipticity of 0.3 at a longer wavelength of 1.8 μm. Besides, we investigate the evolution of supercontinuum at 1.55 μm wavelength for an input pulse width of 25 fs by varying the peak power of the input pulse as well as length of the SN-PCF. The numerical results corroborate that the proposed SN-PCF provides a wider supercontinuum bandwidth for a high input power within a few mm length (2 mm) of fiber. The findings of this work may be useful in ultrahigh-resolution optical coherence tomography and optical communication systems.

1. INTRODUCTION

The supercontinuum generation in photonic crystal fibers (PCFs) has been a topic of intense research ever since it was reported by Ranka et al. [1]. To generate the supercontinuum (SC), the medium should atleast exhibit a flat low anomalous dispersion with a small third order dispersion or zero dispersion [2]. It is obvious that the PCFs operating near a zero dispersion wavelength (ZDW) with higher nonlinearity do not demand large input power for generating the SC. In addition, these desired conditions help smoothen the power spectra of SC [3]. Therefore, highly nonlinear dispersion flattened PCF turns out to be the right candidate for generating SC. Nowadays, the generation of SC in photonic nanowire (PN) have been attracted significant interest with their sub-wavelength diameter due to their unique properties. Such a dielectric waveguides with a nanocore diameter can achieve a tight mode confinement and a strong normal and anomalous waveguide dispersions are combined to allow high nonlinear interactions with the aid of an efficiently designed photonic crystal fiber geometry. Such a photonic device known as photonic crystal fiber nanowire (PCF-NW) has been proposed very recently [4, 5]. These small core PCF structures can be a good candidate for nonlinear applications such as soliton — effect pulse compression and SC generation using very low input power within a short length of fiber [6–9].

In this work, we design a silicon nanowire embedded PCF (SN-PCF) consisting of an elliptical core with equivalent nanowire diameter and a triangular arrangement of air-holes in the cladding and investigate the SC by varying the input peak power and length of the proposed fiber. The paper is laid out as follows. In Section 2, we present the design analysis of the proposed structure. In Section 3, we study the optical properties of the fundamental mode, namely, the group velocity dispersion (GVD), third order dispersion (TOD), birefringence and effective nonlinearity by varying the ellipticity of SN-PCF. Further, we investigate the nonlinear pulse propagation in the anomalous dispersion regime and analyze the evolution of SC at 1.55 μm wavelength with various input powers and various length of SN-PCFs in Section 4. Finally, we summarize the findings in Section 5.

2. DESIGN OF THE PROPOSED SN-PCF

The schematic cross section and mode field distribution of the proposed SN-PCF are as shown in Figs. 1(a) and (b). In the proposed structure, a and b are chosen to be the major and the minor diameters of the elliptical nanocore and the air-hole distribution in the cladding region is composed of 5 rings. In this design, we choose the ellipticity (b/a) value in terms of core diameter (d_c) which is less than 1 μm [10]. The distance between two consecutive air holes (pitch, Λ) is kept at 2 μm and diameter of the air hole (d_h) is 0.7 μm. In this work, we study the optical properties of the

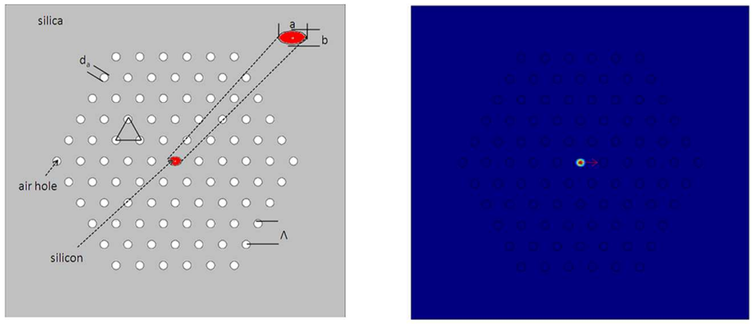

(a) (b)

Figure 1: (a) Geometrical structure and (b) mode field distribution of the proposed SN-PCF with an ellipticity of 0.7.

fundamental mode by increasing the ellipticity values for a range of optical wavelengths from 0.8 to 1.8 μm by keeping a constant value of major core diameter ($a = 550$ nm).

3. WAVEGUIDE DISPERSION

The dispersion is a well known linear effect that depends on the operating wavelength and the nanocore diameter. The diameter dependent GVD and TOD of the x-polarized mode are determined from the effective index of the fundamental mode obtained by finite element method. Fig. 2(a) shows that there is a anomalous GVD for all ellipticity values due to the gradually increase of the field distribution towards the cladding region. When increasing the wavelength, the GVD value increases on the negative side as a result of less confinement within the core and the same trend is observed for all ellipticity values. We achieve a less anomalous GVD of $-0.133\,\mathrm{ps}^2/\mathrm{m}$ for an ellipticity of 0.7 at 0.8 μm wavelength. The variations of TOD with different ellipticity values are shown in Fig. 2(b). Further, we find a almost flattened TOD for all ellipticities up to 1.05 μm wavelength. After increasing the wavelength, we notice that the TOD increases slowly. The proposed fiber exhibits a less TOD ($0.1572 \times 10^{-3}\,\mathrm{ps}^3/\mathrm{m}$) for $b/a = 0.7$ at 0.8 μm wavelength. We achieve a very high birefringence (0.4017) for a smaller ellipticity ($b/a = 0.3$) and lower birefringence (0.0519) for a larger ellipticity ($b/a = 0.7$) at 1.55 μm wavelength as shown in Fig. 3(a). In addition, we notice that the power distribution inside the core decreases rapidly by increasing the ellipticity from 0.3 to 0.7 as is seen in Fig. 3(b). The confinement factor is very high at shorter wavelength (0.8 μm) owing to the tight field confinement within the core. However, at longer wavelength (1.8 μm), the fractional power inside the core is relatively less for a smaller ellipticity of 0.3 due to the large amount of power spreading outside the elliptical nanocore.

4. EFFECTIVE NONLINEARITY

Due to the small core diameter dimensions and the high-index contrast between core and cladding, the air-silicon nanowire exhibits tight mode confinement. Generally, for sub-wavelength nanowire structure, the γ^V value is computed using vectorially-based nonlinear Schrödinger equation (VNSE)

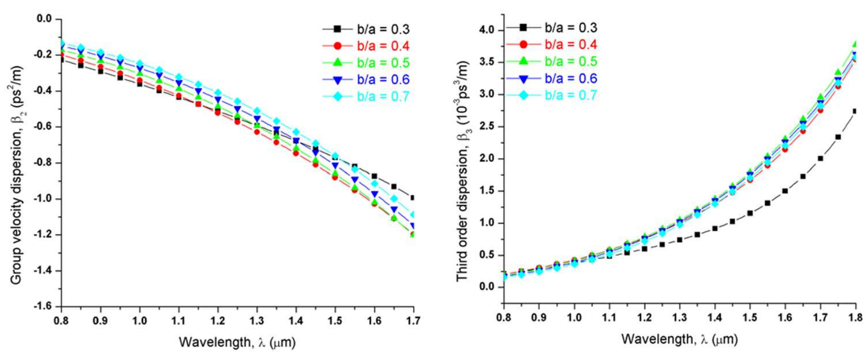

(a) (b)

Figure 2: (a) Group velocity dispersion and (b) third order dispersion of the proposed SN-PCF for various ellipticity.

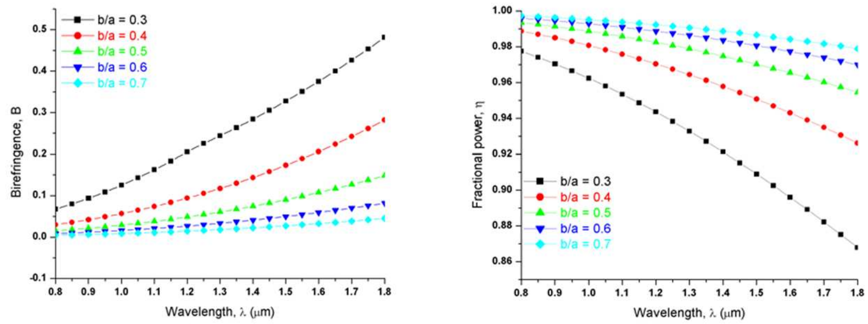

(a) (b)

Figure 3: Variations of (a) birefringence and (b) fractional power of the proposed SN-PCF for various ellipticity.

[11],

$$\gamma^V = k_0 \left(\frac{\epsilon_0}{\mu_0}\right) \frac{\int n_0^2(x,y) n_2(x,y) |e_m|^4 dA}{\left|\int (e_m \times h_m^*) \cdot \hat{z} dA\right|^2}, \tag{1}$$

where k_0, ϵ_0, μ_0 and n_0 are the free space wavenumber, free-space dielectric constant, free space permeability and refractive index of silicon, respectively. Here n_2 is the nonlinear index coefficient ($4.5 \times 10^{-18}\,\mathrm{m}^2/\mathrm{W}$) of silicon whose value is two orders greater than that of silica. The nonlinearity variation of the fundamental mode for different ellipticity values as a function of wavelength is shown in Fig. 4. The small core ellipticity (0.3) exhibits tight mode confinement and very high nonlinearity ($991\,\mathrm{W}^{-1}\mathrm{m}^{-1}$) at $0.8\,\mu\mathrm{m}$ wavelength when compared to other ellipticity values of SN-PCF.

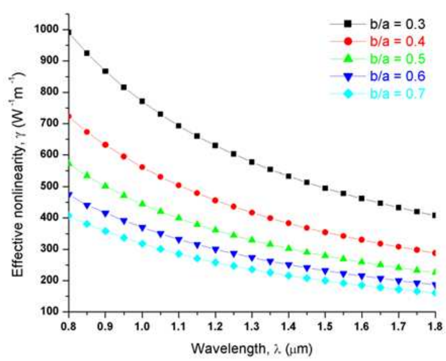

Figure 4: Variation of effective nonlinearity of the SN-PCF for different ellipticity.

5. SIMULATION OF SUPERCONTINUUM GENERATION

The SC generation in the SN-PCF is demonstrated by the generalized nonlinear Schrödinger equation (NLS) with the effects of two-photon absorbtion and free-carrier absorbtion as follows [12],

$$\frac{\partial A}{\partial z} = -\frac{1}{2}\left(\alpha + \alpha^f\right) A - \frac{i}{2}\beta_2 \frac{\partial^2 A}{\partial T^2} + \frac{\beta_3}{6}\frac{\partial^3 A}{\partial T^3} + i\gamma^V \left[1 + \frac{\omega}{\omega_0}\right] A \int_{-\infty}^{\infty} \left[R(T-\tau)|A|^2\right] d\tau \tag{2}$$

where, $A(z,T)$, α, α^f, β_2, β_3, γ^V and $R(T-\tau)$ represent the field envelope, linear loss, free-carrier contribution term, GVD, TOD, effective nonlinearity and Raman response function. In this simulation, we ignore the effect of free carrier absorption, two photon absorption and loss. The nonlinear response function $R(t)$ is defined by [12], $R(t) = (1 - f_R)\delta(t) + f_R h_R(t)$ with $f_R = 0.043$. The delayed Raman response $h_R(t)$ of silicon is expressed as: $h_R(t) = \Omega_R^2 \tau_1 \exp(\frac{-T}{\tau_2}) \sin(\frac{T}{\tau_1})$, where $\tau_1 = 10\,\mathrm{fs}$ and $\tau_2 = 3\,\mathrm{ps}$ correspond to the Raman shift and the bandwidth of the Raman gain spectrum, respectively and Ω_R related to τ_1.

The pulse propagation in SN-PCF is studied by solving the hitherto mentioned NLS type equation using symmetrized split-step Fourier method. We analyze the pulse evolution of SC by considering the hyperbolic secant profile as the input pulse and the same is given by [13]: $A(0,t) = N\sqrt{P_0}\text{sech}[\frac{t}{T_0}]$, where P_0 is the peak power and T_0 is the input soliton duration defined as $T_{\text{FWHM}}/1.763$. The soliton order N is defined as, $N^2 = \frac{\gamma P_0 T_0^2}{|\beta_2|}$. We point out that, in the simulation, we consider the minimum value of ellipticity (0.3) since the proposed SN-PCF meets the requirements (less GVD and high nonlinearity) of SC generation for this value only at 1.55 μm wavelength.

The SC evolution with the pump peak power increasing from 25 to 100 W at 1.55 μm wavelength is as shown in Fig. 5, where the input pulse width is 25 fs and the length of fiber is 2 mm. From the Fig. 5, one can observe that the SN-PCF exhibits a broad spectrum at high input power (100 W) due to the combined action of self-phase modulation, soliton fission and Raman effect. Therefore, the width of the SC depends on the incident power of the pulse. Fig. 6 shows the generation of SC of SN-PCF at 1.55 μm wavelength for various fiber lengths from 5 to 15 mm for a constant input peak power (25 W) and pulse width (25 fs). From Figs. 5 and 6, we observe that the intensity spectrum splits into number of solitons upon increasing the input power and length of the fiber. The proposed SN-PCF exhibits relatively a wider bandwidth of more than 1500 nm. This wider SC spectrum may be useful for ultrahigh-resolution optical coherence tomography system for dental imaging and optical communication systems.

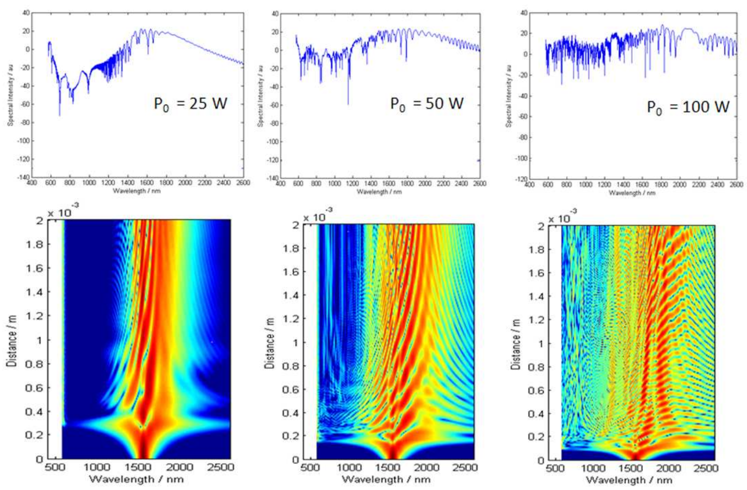

Figure 5: Spectral evolution and spectrum of supercontinuum for various input powers at 1.55 μm wavelength.

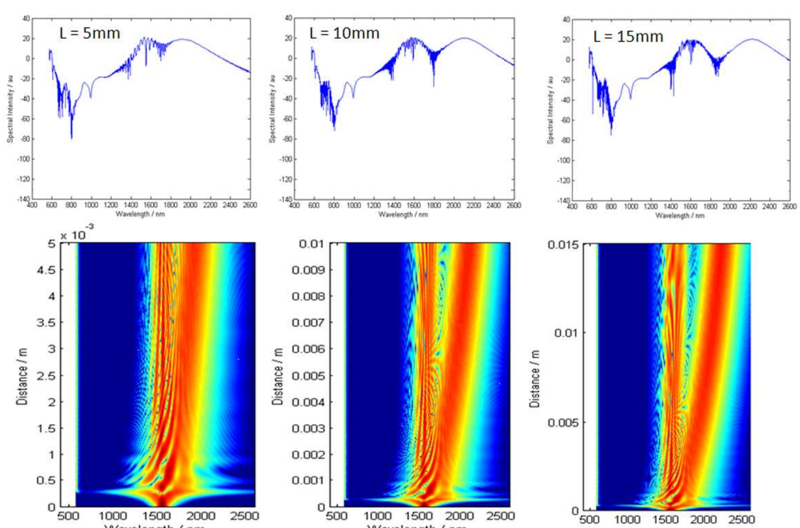

Figure 6: Spectral evolution and spectrum of supercontinuum for various length of SN-PCFs at 1.55 μm wavelength.

6. CONCLUSION

In this paper, we have proposed an elliptical core silicon nanowire embedded photonic crystal fiber and studied the optical properties for various ellipticities using a fully-vectorial finite element method. We have demonstrated the supercontinuum in SN-PCF for various input peak powers and fiber lengths with an input pulse of width 25 fs at 1.55 μm wavelength. We have noticed an enhanced bandwidth of 1800 nm. We envisage that the proposed SN-PCF would highly be useful in the field of medicine, especially, in dentistry, besides its applications in optical communication systems.

ACKNOWLEDGMENT

KSN wishes to thank CSIR [No.: 03(1264)/12/EMR-II] and DST [No.: SR/FTP/PS-66/2009], Government of India, for the financial support through the sponsored projects. SS wishes to thank DST [No.: SR/S2/LOP-0014/2012], Government of India, for the financial support through the sponsored project.

REFERENCES

1. Ranka, J. K., R. S. Windeler, and A. J. Stentz, "Visible continuum generation in air silica microstructure optical fibers with anomalous dispersion at 800 nm," *Opt. Lett.*, Vol. 25, No. 1, 25–27, 2000.
2. Dudley, J. M., G. Genty, and S. Coen, "Supercontinuum generation in photonic crystal fiber," *Rev. Mod. Phys.*, Vol. 78, No. 4, 1135–1184, 2006.
3. Kudlinski, A., G. Bouwmans, M. Douay, M. Taki, and A. Mussot, "Dispersion-engineered photonic crystal fibers for CW-pumped supercontinuum sources," *J. Lightwave Technol.*, Vol. 27, No. 11, 1556–1564, 2009.
4. Biancalana, F., T. X. Tran, S. Stark, M. A. Schmidt, and P. St. J. Russell, "Emergence of geometrical optical nonlinearities in photonic crystal fiber nanowires," *Phys. Rev. Lett.*, Vol. 105, No. 9, 093904–093907, 2010.
5. Gunasundari, E., K. Senthilnathan, S. Sivabalan, M. Abdosllam Abobaker, K. Nakkeeran, and P. Ramesh Babu, "Waveguiding properties of silicon nanowire embedded photonic crystal fiber," *Opt. Materials*, Vol. 36, No. 5, 958–964, 2014.
6. Tong, L., J. Lou, and E. Mazur, "Single-mode guiding properties of sub-wavelength diameter silica and silicon wire waveguides," *Opt. Express*, Vol. 12, No. 6, 1025–1035, 2004.
7. Foster, M., A. L. Gaeta, Q. Cao, and R. Trebino, "Soliton-effect compression of supercontinuum to few-cycle durations in photonic nanowires," *Opt. Express*, Vol. 13, No. 18, 6848–6855, 2005.
8. Salem, A. B., R. Cherif, and M. Zghal, "Low-energy single-optical-cycle soliton self-compression in photonic nanowires," *J. Nnanophoton.*, Vol. 5, No. 1, 059506(1–6), 2011.
9. Salem, A. B., R. Cherif, and M. Zghal, "Soliton-self compression in highly nonlinear chalcogenide photonic nanowires with ulyralow pulse energy," *Opt. Express*, Vol. 19, No. 21, 19955–19966, 2011.
10. Salem, A. B., R. Cherif, and M. Zghal, "Rigorous optical modelling of elliptical photonic nanowires," *J. Lightw. Technol.*, Vol. 30, No. 13, 2176–2180, 2012.
11. Afshar, S. V. and T. M. Monro, "A full vectorial model for pulse propagation in emerging waveguides with subwavelength structures part I: Kerr nonlinearity," *Opt. Express*, Vol. 17, No. 4, 2298–2318, 2009.
12. Yin, L., Q. Lin, and G. P. Agrawal, "Soliton fission and supercontinuum generation in silicon waveguides," *Opt. Lett.*, Vol. 32, No. 4, 391–393, 2007.
13. Agrawal, G. P., *Nonlinear Fiber Optics*, Academic Press, 2007.